Journal of Computational and Applied Mathematics 390 (2021) 113266

Contents lists available at ScienceDirect

Journal of Computational and Applied Mathematics

journal homepage: www.elsevier.com/locate/cam

A shape optimization method for moving interface problems governed by the heat equation ☆

John Lujano, Johannes Tausch *

Department of Mathematics, Southern Methodist University, Dallas, TX 75275, USA

ARTICLE INFO

Article history:
Received 5 February 2019
Received in revised form 27 October 2020

Keywords:
Free boundary problem
Phase transition
Stefan problem
Shape optimization
Integral equation
Heat equation

ABSTRACT

The one dimensional Stefan problem is reformulated as a shape optimization problem for the position of the phase transition as a function of time. The functional to be minimized is the mismatch of the Dirichlet to Neumann map at the moving interface. We show that the minimizer is the only stationary point of the shape functional. A gradient based optimization method is derived using shape calculus. The state and adjoint equations of the heat equation are solved with integral equation techniques which avoid a discretization in the domain. A Nyström quadrature method is analyzed and numerical results are presented.

1. Introduction

Melting and solidification problems with either planar or spherical geometry arise in many applications of material science. Often, such processes are accurately modeled by a one dimensional Stefan problem. This is a well-studied topic and we refer to, e.g., [1–3] for an overview of the engineering and mathematical literature. Here, the evolution of the phase change is governed by the Stefan condition which states that the heat flux at the interface is proportional to the interface velocity.

The Stefan problem is an important example of a free surface problem where in addition to the temperature distribution the position of the phase transition is a-priori unknown. The literature on analytical and numerical methods for this type of problem is too extensive to review here in detail. To put this paper in context we only mention two different classes of numerical techniques and a few representative papers.

The first class is the front-tracking method. Assuming the solution for some time $t > 0$ has been computed, the Stefan condition is used to determine the velocity at t, and hence the future position of the interface. This results in an ODE-type solver for the interface. While explicit solvers are fairly straightforward to implement, they are generally stable only for low order time stepping. Implicit solvers have better stability but are more difficult to implement because a nonlinear equation must be solved in each time step. Several variations of front tracking methods have appeared, the main difference is how the heat equation in the bulk is solved. This can be either finite differences [4–6], the heat balance integral method [7] or boundary integral equations [8,9]. In this work we also employ integral equation methods to solve the parabolic PDE. This approach eliminates the need to discretize the domain and avoids dealing with remeshing the domain in each time step.

The second class of techniques for free surface problems is the level set method. Here the interface is implicitly defined by the zero-level of an auxiliary function. In the case of moving geometries, this function satisfies the Hamilton–Jacobi

☆ This material is based upon work supported by the National Science Foundation, United States under grant DMS-1720431.
* Corresponding author.
E-mail addresses: jlujano@mail.smu.edu (J. Lujano), tausch@smu.edu (J. Tausch).

https://doi.org/10.1016/j.cam.2020.113266
0377-0427/

equation, a hyperbolic PDE, which is coupled with the parabolic equation for the temperature. This idea has generated considerable interest [10,11], however, we do not consider it in this work as the Hamilton–Jacobi equation is not tractable with integral equation methods.

This paper approaches the Stefan problem from the viewpoint of shape optimization. Here the goal is to determine a domain that minimizes an objective function which is often constrained by a PDE [12–14]. There has been considerable interest to use shape optimization for stationary free boundary problems of elliptic problems, and in the convergence of their discretization. The papers [15–17] are representative examples. The literature on shape optimization for parabolic equations is much sparser. However, there are recent papers that deal with the reconstruction of the shape of an interior inclusion from time dependent, overdetermined Cauchy data on an exterior boundary [18–20].

Unlike the inverse shape reconstruction, the Stefan problem is not ill-posed, but is nevertheless challenging because of the time dependence of the geometry. In [21] an error functional was defined that assigns to an arbitrary evolution of the interface the mismatch between the Neumann data and the Stefan condition. The solution of the Stefan problem is the minimizer of this functional. In this article, we present a numerical method to compute the minimum via gradient-based optimization techniques. Hence we will derive the shape calculus to determine the derivative of the solution to the heat equation with respect to changing the time-dependent interface. Further, we will derive an adjoint equation to compute the shape gradient efficiently. With the help of the adjoint, we will show that the only stationary point of the error functional is the minimum solution. The practical consequence is that a steepest-descent type algorithm cannot terminate in a local minimum that is not the desired solution.

To solve the state and adjoint equation efficiently and with high accuracy we will derive an integral equation reformulation for boundary values of the heat equation. Here special attention must be given to additional terms that arise because of time dependent geometries. We present a Nyström quadrature method that handles singularities in the integral operators and the solution. Finally, we present numerical examples to confirm the practicality of our approach.

2. Mathematical formulation

We consider the classical Stefan problem, which describes the melting of a block of ice which initially occupies a half-space. Melting is induced by applying a heat source at the end. After non-dimensionalization of the space and time variables, the problem can be stated in terms of the heat equation for temperature $U(x,t)$ in the liquid phase

$$\begin{aligned} \partial_t U(x,t) - \partial_x^2 U(x,t) &= 0, && x \in (0,R(t)),\ t \in (0,T),\\ \partial_x U(0,t) &= -f(t), && t \in (0,T),\\ U(R(t),t) &= 0, && t \in (0,T),\\ R'(t) + \partial_x U(R(t),t) &= 0, && t \in (0,T),\\ R(0) &= 0. \end{aligned} \tag{2.1}$$

The goal is to determine the position of the solid–liquid interface $R(t)$ for the time interval $t \in (0,T)$. Here we assume that $R(0) = 0$, thus the initial domain is empty and we do not have to supply an initial temperature for the melt. The Neumann data $f(t)$ reflects the heating at $x = 0$. The Dirichlet condition at $x = R(t)$ states that the temperature of the liquid at the interface is equal to the melting temperature. The third boundary condition is the Stefan condition, which states that the velocity of the interface is proportional to the heat flux on the interface.

This is a well posed problem in the sense that there is a unique solution $R(t)$ which depends continuously on the data $f(t)$. For a nice introduction to the solvability theory of (2.1) we refer to [22].

In this work we employ shape optimization techniques to compute the function $R(t)$ numerically. We begin by defining an error functional. To that end we replace the actual position of the interface $R(t)$ by the guess $r(t)$ which satisfies $r(0) = 0$, and solve the heat equation with the Neumann condition at $x = 0$ and Dirichlet condition at $x = r(t)$.

$$\begin{aligned} \partial_t u(x,t) - \partial_x^2 u(x,t) &= 0, && (x,t) \in \Omega_{T,r},\\ \partial_x u(0,t) &= -f(t), && t \in (0,T),\\ u(r(t),t) &= 0, && t \in (0,T). \end{aligned} \tag{2.2}$$

Here, $\Omega_{T,r}$ denotes the space–time domain

$$\Omega_{T,r} := \{(x,t) :\ 0 < x < r(t),\ 0 < t < T\}.$$

Eq. (2.2) will be referred to as the state equation. Since the function $r(t)$ has been a guess, one cannot expect that the Stefan condition is satisfied. The quality of the guess is measured in terms of the shape functional

$$J(r) = \frac{1}{2}\int_0^T \left[r'(t) + \partial_x u(r(t),t)\right]^2 dt. \tag{2.3}$$

The shape optimization method is based on minimizing

$$R \equiv \min_{r(0)=0} J(r). \tag{2.4}$$

Clearly, the solution $R(t)$ of (2.1) is the minimizer of (2.4) that satisfies $J(R) = 0$, and vice versa, if $J(R) = 0$ is the minimizer, then $R(t)$ solves (2.1). We will use a gradient-based iteration to solve the minimization problem (2.4). To derive the shape gradient, we have to consider the change of the functional (2.3) if $r(t)$ is replaced by the perturbed interface $r(t) + \epsilon\widehat{r}(t)$. Here $\widehat{r}(t)$ is another differentiable function with $\widehat{r}(0) = 0$. For a sufficiently small $\epsilon > 0$ consider the parameterized heat equation

$$\begin{aligned} \partial_t u(x,t,\epsilon) - \partial_x^2 u(x,t,\epsilon) &= 0, && (x,t) \in \Omega_{T,r+\epsilon\widehat{r}} \\ \partial_x u(0,t,\epsilon) &= -f(t), && t \in (0,T), \\ u(r(t)+\epsilon\widehat{r}(t),t,\epsilon) &= 0, && t \in (0,T). \end{aligned}$$

The derivative with respect to ϵ is the sensitivity of the solution with respect to changing the boundary curve. We set

$$\delta u(x,t) = \frac{\partial}{\partial\epsilon} u(x,t,\epsilon)\Big|_{\epsilon=0}.$$

This derivative satisfies the heat equation

$$\begin{aligned} \partial_t \delta u(x,t) - \partial_x^2 \delta u(x,t) &= 0, && (x,t) \in \Omega_{T,r}, \\ \partial_x \delta u(0,t,\epsilon) &= 0, && t \in (0,T), \\ \delta u(r(t),t) &= -\partial_x u(r(t),t)\widehat{r}(t), && t \in (0,T). \end{aligned} \tag{2.5}$$

The Dirichlet condition on $x = r(t)$ follows from the multivariate chain rule.

Another application of the chain rule shows that the change of the error functional is

$$\delta J[\widehat{r}](r) := \frac{d}{d\epsilon} J(r+\epsilon\widehat{r})\Big|_{\epsilon=0} = \int_0^T \Big(\partial_x u + r'\Big)\Big(\partial_x^2 u\,\widehat{r} + \partial_x \delta u + \widehat{r}'\Big)\,dt,$$

where $\partial_x u$, $\partial_x^2 u$ and $\partial_x \delta u$ are evaluated at $(x,t) = (r(t),t)$.

The above expression contains a second derivative, but it can be reduced to an equivalent expression involving only first order derivative as follows. Differentiating the Dirichlet condition in the state equation (2.2) with respect to time gives

$$\partial_x u(r(t),t)\,r'(t) + \partial_t u(r(t),t) = 0,$$

and since u satisfies the heat equation

$$\partial_x^2 u(r(t),t) = \partial_t u(r(t),t) = -\partial_x u(r(t),t)\,r'(t)$$

holds. Thus the change of the error functional is

$$\begin{aligned} \delta J[\widehat{r}](r) &= \int_0^T \Big(\partial_x u + r'\Big)\Big(\partial_x \delta u - \partial_x u\, r'\widehat{r} + \widehat{r}'\Big)\,dt, \\ &= \int_0^T \Big(\partial_x u + r'\Big)\Big(\partial_x \delta u + \delta u\, r' + \widehat{r}'\Big)\,dt. \end{aligned} \tag{2.6}$$

3. Adjoint formulation

Choosing an n-dimensional vector space and a basis for the discretization of r and $\widehat{r}$ reduces (2.4) to a nonlinear optimization problem in n variables. The partial derivatives with respect to the basis coefficients are obtained by replacing $\widehat{r}$ in (2.6) by each basis function. Thus the computation of the complete gradient for a given $r(t)$ involves solving (2.5) n times, which has to be performed in each step of a gradient-based optimization method.

Fortunately this large computational overhead can be reduced by a trick that is well known for PDE constrained optimization problems. The idea is to express the derivative $\delta J[\widehat{r}](r)$ in terms of an adjoint equation to (2.5). To describe how this trick can be applied to the problem at hand we need the following formula for the time-derivative of a spatial integral with time-varying bounds

$$\frac{d}{dt}\int_0^{r(t)} f(x,t)\,dx = \int_0^{r(t)} \partial_t f(x,t)\,dx + f(r(t),t)r'(t). \tag{3.1}$$

Suppose now that v is a solution of the heat equation in $\Omega_{T,r}$ and p is a solution of the backward heat equation

$$\begin{aligned} -\partial_t p(x,t) - \partial_x^2 p(x,t) &= 0, && (x,t) \in \Omega_{T,r}, \\ p(x,T) &= 0, && x \in (0, r(T)). \end{aligned}$$

Note that for well posedness terminal conditions instead of initial conditions are supplied. Using (3.1), the fundamental theorem of calculus and integration by parts the following form of Green's second identity in $\Omega_{T,r}$ can be derived.

$$\begin{aligned} 0 &= \int_0^T \int_0^{r(t)} \Big(\partial_t v - \partial_x^2 v\Big) p + \Big(\partial_t p + \partial_x^2 p\Big) v \, dx dt, \\ &= \int_0^T \int_0^{r(t)} \partial_t \Big(pv\Big) \, dx dt + \int_0^T \int_0^{r(t)} \partial_x^2 p \, v - \partial_x^2 v \, p \, dx dt, \\ &= \int_0^T \Big[\partial_x p \, v - p \, \partial_x v\Big]_{x=0}^{r(t)} dt - \int_0^T v p r' \Big|_{x=r(t)} dt. \end{aligned} \tag{3.2}$$

Now we get more specific about the functions v and p. We replace v by the solution δu of (2.5). In addition, we let the Dirichlet data of p be the mismatch in the definition of the functional (2.3). Thus p solves

$$\begin{aligned} -\partial_t p(x,t) - \partial_x^2 p(x,t) &= 0, && (x,t) \in \Omega_{T,r}, \\ \partial_x p(0,t) &= 0, && t \in (0,T), \\ p(r(t),t) &= r'(t) + \partial_x u(r(t),t), && t \in (0,T), \\ p(x,T) &= 0, && x \in (0, r(T)). \end{aligned} \tag{3.3}$$

From this and (3.2) we can conclude that

$$\int_0^T p\Big(\partial_x \delta u + \delta u \, r'\Big) \, dt = \int_0^T \partial_x p \, \delta u \, dt \tag{3.4}$$

where the functions are evaluated at $x = r(t)$.

Using the adjoint equations (3.3) and (3.4) the derivative of the error function (2.6) can be expressed as

$$\begin{aligned} \delta J[\widehat{r}](r) &= \int_0^T p\Big(\partial_x \delta u + \delta u \, r' + \widehat{r}'\Big) \, dt \\ &= \int_0^T \partial_x p \delta u + p\widehat{r}' \, dt. \end{aligned}$$

Since $\delta u = -\widehat{r}\partial_x u$ this expression becomes

$$\delta J[\widehat{r}](r) = \int_0^T p\widehat{r}' - \partial_x p \, \partial_x u \widehat{r} \, dt. \tag{3.5}$$

Eq. (3.5) involves only solutions of the state equation (2.2) and adjoint equation (3.3). This is advantageous when computing the gradient of the shape functional, because this eliminates the need to solve the equation for the shape derivative (2.5) for every basis function.

Since it will be used later on, we will state the time-reversed adjoint equation. Setting $\breve{p}(x,t) := p(x, T-t)$ we obtain from (3.3)

$$\begin{aligned} \partial_t \breve{p}(x,t) - \partial_x^2 \breve{p}(x,t) &= 0, && (x,t) \in \breve{\Omega}_{T,r}, \\ \partial_x \breve{p}(0,t) &= 0, && t \in (0,T), \\ \breve{p}(r(t),t) &= \breve{p}(t), && t \in (0,T), \\ \breve{p}(x,0) &= 0, && x \in (0, r(T)). \end{aligned} \tag{3.6}$$

where $\breve{p}(t) = r'(T-t) + \partial_x u(r(T-t), T-t)$ and $\breve{\Omega}_{r,T} = \Omega_{r(T-\cdot),T}$. For general $p(t)$ this equation has two possible singularities, namely, the Dirichlet condition at $t = 0$ may be incompatible with the initial condition, and the domain $\breve{\Omega}_{r,T}$ collapses into a point at $t = T$. This will be important for the numerical solution via integral equations which will be discussed in Section 4.

The adjoint formulation is also useful to extract some information about the nature of the optimization problem (2.4). We will show that the minimum is the only stationary point. This has the practical consequence that a steepest descent type algorithm cannot get stuck in a local minimum that is not the solution of the Stefan problem.

Theorem 3.1. *If $f(t) > 0$ and $\delta J[\widehat{r}](r) = 0$ for all C^1-functions $\widehat{r}$ with $\widehat{r}(0) = 0$ then $r = R$.*

Proof. Integrating of the first term of (3.5) by parts gives

$$\delta J[\widehat{r}](r) = p(T)\widehat{r}(T) - \int_0^T \Big(p' + \partial_x p \partial_x u\Big)\widehat{r} \, dt$$

where $p'(t) = \frac{d}{dt}p(r(t), t)$ and hence the assumption $\delta J[\widehat{r}](r) = 0$ implies that

$$p' = -\partial_x u \partial_x p, \tag{3.7}$$

$$p(T) = 0. \tag{3.8}$$

Further, it is shown in [22] that $\partial_x u(r(t), t) < 0$ when $t > 0$, so p' and $\partial_x p$ have the same sign.

Recall that $\breve{p}(x, t) = p(x, T - t)$ solves the heat equation (3.6). First note that $\breve{p}$ cannot have strict extrema on the boundaries $x = 0$, and $x = r(t)$, $0 < t < T$. If there was an extremum then the parabolic Hopf lemma [23] states that the derivative $\partial_x \breve{p}$ is non-zero. However, on $x = 0$ the Neumann condition $\partial_x \breve{p} = 0$ is imposed and thus no extremum can occur. If there was an extremum on the boundary $x = r(t)$, say, at $t = t^* \in (0, T)$, then $\breve{p}'(t^*) = 0$ and then we can conclude from (3.7) that $\partial_x \breve{p} = \partial_x p = 0$ because $\partial_x u < 0$. Again, this contradicts Hopf's lemma and hence there is no extremum on $x = r(t)$.

Thus the only possibility for a strict extremum of $\breve{p}$ is the point $(x, t) = (0, T)$. Suppose now that $\breve{p}(0, T) > 0$ is a strict maximum which implies that the line $\breve{p}(\cdot, 0) = 0$ is a minimum. We also have $\breve{p}' \geq 0$ and by continuity there must be a $t^* \in (0, T)$ such that $\breve{p}'(t^*) > 0$. Set $\widetilde{p}(x, t) = \breve{p}(t) - \breve{p}(x, t)$, this function satisfies

$$\begin{aligned}
\partial_t \widetilde{p}(x, t) - \partial_x^2 \widetilde{p}(x, t) &= \breve{p}'(t), && (x, t) \in \breve{\Omega}_{T,r}, \\
\partial_x \widetilde{p}(0, t) &= 0, && t \in (0, T), \\
\widetilde{p}(r(t), t) &= 0, && t \in (0, T), \\
\widetilde{p}(x, 0) &= 0, && x \in (0, r(T)),
\end{aligned}$$

It follows from the strong minimum principle that $\widetilde{p}(x, t) > 0$ in the domain $\Omega_{T,r} \cap \{(x, t) : t > t^*\}$ and therefore $\partial_x \widetilde{p} < 0$ for $x = r(t)$, $t > t^*$. On the other hand, with the above transformation condition (3.7) appears as $\breve{p}' = -\partial_x u \partial_x \widetilde{p}_x$, and since $-\partial_x u > 0$ we have $\breve{p}' < 0$. This is a conflict with the fact that $\breve{p}'$ is a monotonically increasing function. Therefore $\breve{p}(0, T) > 0$ cannot be a maximum. The same argument, with opposite signs, implies that $\breve{p}(0, T) < 0$ also leads to a contradiction. Thus $\breve{p}(0, T) = 0$ and therefore $\breve{p}$ vanishes in $\breve{\Omega}_{T,r}$.

We can conclude that $p = 0$ is the only solution of the adjoint equation that also satisfies (3.7) and (3.8). In this case $\partial_x u = -r'$ is the solution of the Stefan problem.

4. Integral formulations

Since the state and adjoint equations have to be solved repeatedly in a minimization procedure it is important to use efficient solution methods. We will consider an integral approach, which is equivalent to the boundary integral method for parabolic problems in higher space dimensions. We will see that in the case of one space dimension the heat equation can be reduced to an Abel-type integral equation in time.

The free space Green's function for the one dimensional heat equation is

$$G_f(x, y, t, \tau) = \frac{1}{\sqrt{4\pi(t - \tau)}} \exp\left(-\frac{(x - y)^2}{4(t - \tau)}\right)$$

which satisfies the time reversed equation

$$-\partial_\tau G_f(x, y, t, \tau) - \partial_y^2 G_f(x, y, t, \tau) = \delta(t - \tau)\,\delta(x - y).$$

Since the state and adjoint equations involve the boundary $y = 0$, it is convenient to use the method of images. Hence we consider the kernel

$$\begin{aligned}
G_i(x, y, t, \tau) &= G_f(x, y, t, \tau) + G_f(x, -y, t, \tau) \\
&= \frac{1}{\sqrt{4\pi(t - \tau)}} \left[\exp\left(-\frac{(x - y)^2}{4(t - \tau)}\right) + \exp\left(-\frac{(x + y)^2}{4(t - \tau)}\right)\right].
\end{aligned}$$

Note that $\partial_y G_i(x, 0, t, \tau) = 0$.

The integral formulations depend on the thermal single and double layer potentials. For a function $\varphi \in C^0[0, T]$ they are defined as

$$\widetilde{\mathcal{V}}\varphi(x, t) = \int_0^t G_i(x, r(\tau), t, \tau)\varphi(\tau)\, d\tau, \tag{4.1}$$

$$\widetilde{\mathcal{K}}\varphi(x, t) = \int_0^t \partial_y G_i(x, r(\tau), t, \tau)\varphi(\tau)\, d\tau, \tag{4.2}$$

$$\widetilde{\mathcal{V}}_0\varphi(x, t) = \int_0^t G_i(x, 0, t, \tau)\varphi(\tau)\, d\tau. \tag{4.3}$$

Note that $\widetilde{\mathcal{V}}$ and $\widetilde{\mathcal{K}}$ are potentials generated by the interface $y = r(\tau)$ while $\widetilde{\mathcal{V}}_0$ comes from the boundary $y = 0$. For an evaluation point (x, t) in the interior of the space–time domain $\Omega_{T,r}$ all three potentials are smooth functions that solve the heat equation.

For a solution u of the heat equation with homogeneous Neumann boundary conditions we write for the boundary data

$$u(\tau) = u(r(\tau), \tau) \quad \text{and} \quad q(\tau) = \partial_x u(r(\tau), \tau) + r'(\tau)u(\tau).$$

Then the Green's representation formula is

$$u(x, t) = \widetilde{\mathcal{V}} q(x, t) - \widetilde{\mathcal{K}} u(x, t) + \widetilde{\mathcal{V}}_0 f(x, t), \quad (x, t) \in \Omega_{T,r}.$$

The benefit of using the method of images is that the above formula does not include the Dirichlet data of u on the boundary $y = 0$.

The integral equations for the boundary value problems of the heat equation can be obtained by taking the limit as $x \to r(t)$ and using the usual jump relations of the layer potentials. It is not difficult to check that these relations remain valid when the boundary is time dependent. Thus we have

$$\frac{1}{2}u(t) = \mathcal{V} q(t) - \mathcal{K} u(t) + \mathcal{V}_0 f(t), \tag{4.4}$$

where the operators $\mathcal{V}$, $\mathcal{K}$ and $\mathcal{V}_0$ are defined as in (4.1)–(4.3) but with x replaced by $r(t)$. In this case the integrals in (4.1) and (4.2) have a $O((t-\tau)^{-\frac{1}{2}})$ singularity at the right endpoint of integration.

4.1. State equation

The state equation has vanishing Dirichlet conditions on $x = r(t)$, thus (4.4) becomes

$$\mathcal{V} q_s(t) = -\mathcal{V}_0 f(t), \tag{4.5}$$

where $q_s(t) = \partial_y u(r(t), t)$ is the normal derivative on the boundary $y = r(\tau)$. Because of the singularity of the kernel, (4.5) is a generalized Abel equation.

4.2. Adjoint equation

An integral formulation of the adjoint equation can be derived from the time-reversed equation (3.6) and the Green's representation formula (4.4). Since the Neumann condition at $x = 0$ vanishes we get

$$\check{\mathcal{V}} \check{q}_a(t) = \frac{1}{2}\check{p}(t) + \check{\mathcal{K}} \check{p}(t), \quad t \in [0, T], \tag{4.6}$$

where $\check{\mathcal{V}}$ and $\check{\mathcal{K}}$ denote the layer potentials for the time-reversed interface position $\check{r}$. The unknown q_a is

$$\check{q}_a(t) = \partial_x p(\check{r}(t), T - t) - p(\check{r}(t), T - t)\check{r}'(t).$$

5. Discretization of thermal potentials

The integral operator $\mathcal{V}$ in (4.5) is a generalized Abel integral operator because it can be written in the form

$$\mathcal{V} q(t) = \int_0^t \frac{1}{\sqrt{t - \tau}} k(t, \tau) q(\tau)\, d\tau$$

with the kernel

$$k(t, \tau) = \frac{1}{\sqrt{4\pi}} \left[\exp\left(-\frac{(r(t) - r(\tau))^2}{t - \tau} \right) + \exp\left(-\frac{(r(t) + r(\tau))^2}{t - \tau} \right) \right].$$

Since

$$r(t) - r(\tau) = (t - \tau) r_1(t, \tau),$$
$$r(t) + r(\tau) = 2r(t) - (t - \tau) r_1(t, \tau),$$

it follows that $k(t, t) = 1/\sqrt{4\pi}$ as long as $t > 0$. However, the limit of $k(t, 0)$ as t approaches zero is $1/\sqrt{\pi}$ because $r(t) \sim t$ results in a non-trivial contribution of the second term. Thus $k(t, \tau)$ is only smooth in the interior of the triangle

$$\sigma_T := \{(t, \tau), 0 \le \tau \le t \le T\}$$

and has a discontinuity in the origin. Likewise, the time reversed operator $\check{\mathcal{V}}$ in (4.6) has a singularity at $(t, \tau) = (T, T)$ since $\check{r}(T) = 0$.

Therefore discretization methods for the Abel integral equation must be modified to obtain the expected convergence results. Our approach is a modification of the singularity subtraction method in [24]. To this end we introduce the additional variable $s = t - \tau$ in the kernel of $\mathcal{V}$ by writing

$$\begin{aligned} G_i(r(t), r(\tau), t, \tau) &=: \frac{1}{\sqrt{s}}\, k(t, \tau, s) \\ &= \frac{1}{\sqrt{s}} \left[k_1(t, \tau) + \exp\left(-\frac{r^2(t)}{s}\right) k_2(t, \tau) \right] \end{aligned} \tag{5.1}$$

where

$$\begin{aligned} k_1(t, \tau) &= \frac{1}{\sqrt{4\pi}} \exp\left(-(t-\tau)\frac{r_1^2(t, \tau)}{4}\right), \\ k_2(t, \tau) &= \frac{1}{\sqrt{4\pi}} \exp\left(r(t) r_1(t, \tau) - \frac{t-\tau}{4} r_1^2(t, \tau)\right). \end{aligned}$$

For the time reversed $\check{\mathcal{V}}$ simply replace r by $\check{r}$. The singularity subtraction is based on the decomposition

$$\mathcal{V}q(t) = \int_0^t \frac{1}{\sqrt{t-\tau}} \Big[k(t, \tau, t-\tau) q(\tau) - k(t, t, t-\tau) q(t) \Big]\, d\tau + K(t) q(t) \tag{5.2}$$

where the function $K(t)$ can be expressed in closed form

$$\begin{aligned} K(t) &= \int_0^t \frac{k(t, t, t-\tau)}{\sqrt{t-\tau}} d\tau \\ &= \frac{1}{\sqrt{4\pi}} \int_0^t \frac{1}{\sqrt{(t-\tau)}} \left[1 + \exp\left(-\frac{r^2(t)}{t-\tau}\right) \exp\big(r(t) r'(t)\big) \right] d\tau \\ &= \frac{\sqrt{t}}{\sqrt{\pi}} \left[1 + \exp\left(-\frac{r^2(t)}{t}\right) - r(t)\, \mathrm{erfc}\left(\frac{r(t)}{\sqrt{t}}\right) \exp\big(r(t) r'(t)\big) \right]. \end{aligned}$$

Below we will show that the difference in the first integral is a sufficiently regular function that vanishes for $t = \tau$. Hence the singularity is canceled and the trapezoidal rule becomes

$$\begin{aligned} \mathcal{V}q(t_n) \approx h \sum_{j=0}^{n-1}{}' \frac{1}{\sqrt{t_n - t_j}} \Big[k(t_n, t_j, t_n - t_j) q(t_j) - k(t_n, t_n, t_n - t_j) q(t_n) \Big] \\ + K(t_n) q(t_n) \end{aligned}$$

where $h = T/M$ is the step size, M the total number of time steps, $t_j = jh$ and the primed summation sign indicates that the first term is multiplied by $\frac{1}{2}$. Sorting out the $q(t_n)$'s leads to the quadrature rule

$$\mathcal{V}^h q(t_n) := h \sum_{j=0}^{n-1}{}' \frac{k(t_n, t_j, t_n - t_j)}{\sqrt{t_n - t_j}} q(t_j) + \mu_n q(t_n)$$

where

$$\widetilde{\mu}_n = K(t_n) - h \sum_{j=1}^{n-1}{}' \frac{k(t_n, t_n, t_n - t_j)}{\sqrt{t_n - t_j}}$$

The convergence of the Nyström method depends on the following quadrature error.

Lemma 5.1. *If $r(t)$ and $q(t)$ are sufficiently smooth then*

$$\big| \mathcal{V}q(t_n) - \mathcal{V}^h q(t_n) \big| = O(h^{\frac{3}{2}}).$$

Proof. If the integrand in (5.2) is denoted by $f(t, \tau)$ then the quadrature error of the trapezoidal rule is

$$\mathcal{V}q(t_n) - \mathcal{V}^h q(t_n) = h^2 \int_0^{t_n} \frac{\partial^2 f}{\partial \tau^2}(t_n, \tau) B\left(\frac{\tau}{h}\right) d\tau \tag{5.3}$$

where B is the Peano kernel, given by

$$B(x) = \frac{1}{12}x(1-x), \quad \text{for } x \in [0,1],$$

and extended periodically to all of $\mathbb{R}$. The main technical part of the argument consists of estimating the second derivative. From (5.1) we can write

$$f(t,\tau) = \frac{1}{\sqrt{s}}\Big[k_1(t,\tau)q(\tau) - k_1(t,t)q(t)\Big] + \frac{1}{\sqrt{s}}\exp\left(-\frac{r^2(t)}{s}\right)\Big[k_2(t,\tau)q(\tau) - k_2(t,t)q(t)\Big]$$

where $s = t-\tau$. Since $\tau \to k_i(t,\tau)q(\tau)$, $i = 1,2$ are smooth functions there are smooth functions f_i such that $k_i(t,\tau)q(\tau) - k_i(t,t)q(t) = sf_i(t,\tau)$ and hence

$$f(t,\tau) = \sqrt{s}f_1(t,\tau) + \sqrt{s}\exp\left(-\frac{r^2(t)}{s}\right)f_2(t,\tau)$$

Simple differentiation shows that there is a constant M_1 such that

$$\frac{\partial}{\partial s}\left[\sqrt{s}\exp\left(-\frac{r^2}{s}\right)\right] = \left(\frac{r^2}{s^{\frac{3}{2}}} + \frac{1}{2\sqrt{s}}\right)\exp\left(-\frac{r^2}{s}\right) \le \frac{M_1}{\sqrt{s}}$$

because $x\exp(-x)$ is bounded for $x \ge 0$. Likewise,

$$\frac{\partial^2}{\partial s^2}\left[\sqrt{s}\exp\left(-\frac{r^2}{s}\right)\right] \le \frac{M_2}{s^{\frac{3}{2}}}.$$

Since the derivatives of f_1 and f_2 are bounded we obtain from the product rule

$$\left|\frac{\partial^2 f}{\partial \tau^2}(t_n,\tau)\right| \le \frac{C}{s^{\frac{3}{2}}}.$$

In [24] it is shown that for $\alpha, \beta > -2$, there is a constant $C > 0$ such that

$$\int_0^{nh}(nh-\tau)^\alpha \tau^\beta B\left(\frac{\tau}{h}\right)d\tau \le C\,t^{1+\alpha+\beta}\left(1 + \frac{1}{n^{\alpha+1}} + \frac{1}{n^{\beta+1}}\right).$$

Specializing this result to $\alpha = -3/2$ and $\beta = 0$ shows that the integral in (5.3) is $O(h^{-\frac{1}{2}})$ which completes the proof.

Next consider a potential with a density of the form $\varphi(t) = t^{-\frac{1}{2}}\widetilde{\varphi}(t)$. To handle the singularities on both endpoints add and subtract the linear interpolation of the integrand. Thus

$$\int_0^t \frac{1}{\sqrt{t-\tau}}\frac{1}{\sqrt{\tau}}\Big[k(t,\tau,t-\tau)\widetilde{\varphi}(\tau) - L(t,\tau,t-\tau)\Big]d\tau + K_0(t)\widetilde{\varphi}(0) + K_1(t)\widetilde{\varphi}(t)$$

where

$$L(t,\tau) = \frac{1}{t}\Big[k(t,t,t-\tau)\tau\widetilde{\varphi}(t) + k(t,0,t-\tau)(t-\tau)\widetilde{\varphi}(0)\Big].$$

and

$$K_0(t) = \frac{1}{t}\int_0^t \frac{\sqrt{t-\tau}}{\sqrt{\tau}}k(t,0,t-\tau)\,d\tau,$$
$$K_1(t) = \frac{1}{t}\int_0^t \frac{\sqrt{\tau}}{\sqrt{t-\tau}}k(t,t,t-\tau)\,d\tau.$$

The first integral is nonsingular and is replaced by the trapezoidal rule. Sorting out the $\varphi(t_j)$ terms leads to the quadrature rule

$$I(t_n) = \mu_n^{(0)}\widetilde{\varphi}(0) + h\sum_{j=1}^{n-1}\frac{k(t_n,t_j,t_n-t_j)}{\sqrt{t_n-t_j}}\varphi(t_j) + \mu_n^{(1)}\widetilde{\varphi}(t_n) + O(h^{\frac{3}{2}}),$$

where

$$\widetilde{\mu}_n^{(0)} = K_0(t_n) - h\sum_{j=1}^{n-1}\frac{k(t_n,t_j,t_n-t_j)}{\sqrt{t_n-t_j}\sqrt{t_j}},$$

$$\widetilde{\mu}_n^{(1)} = K_1(t_n) - h\sum_{j=1}^{n-1}\frac{k(t_n,t_n,t_n-t_j)}{\sqrt{t_n-t_j}\sqrt{t_j}}.$$

Table 1
Final functional value and maximum error of interface position for the example in Section 6.1. M is the number of time steps of the integral equation solver.

M	Functional	Order	Error	Order
20	3.74e−07		2.55e−04	
40	4.30e−08	3.12	7.53e−05	1.76
80	5.26e−09	3.03	2.21e−05	1.77
160	1.01e−09	2.38	7.20e−06	1.62
320	1.74e−10	2.54	2.48e−06	1.54
640	2.59e−11	2.74	8.49e−07	1.55
1280	3.59e−12	2.85	2.91e−07	1.54

Since the singularity removed integrand is of order $\sqrt{t-\tau}\sqrt{\tau}$ at the endpoints the convergence rate is only $O(h^{\frac{3}{2}})$ instead of the $O(h^2)$ rate for the trapezoidal rule for smooth integrands. The proof is completely analogous to the above proof and is omitted.

6. Numerical results

We give more details about the discretization of the optimization problem (2.4). We seek an approximation $r_N(t)$ of the unknown function $r(t)$ in a finite dimensional vector space of functions that satisfy the initial condition $r(0) = 0$. If $\varphi_i(t)$ is a basis for this vector space, then $r_N(t)$ and the perturbation $\widehat{r}(t)$ are linear combinations of the basis functions

$$r_N(t) = \sum_{j=0}^{N} r_j \varphi_j(t), \quad \widehat{r}_N(t) = \sum_{j=0}^{N} a_i \varphi_j(t). \tag{6.1}$$

Thus the problem (2.4) is replaced by the optimization problem in $\mathbb{R}^{N+1}$

$$R_N \equiv \min_{[r_0,\dots,r_N]\in\mathbb{R}^{N+1}} J(r_N),$$

and the minimization procedure is

Choose an initial guess $r_N(t)$
repeat
Solve the state equation (2.2)
Compute the error functional $J(r_N)$ in (2.3).
Solve the adjoint equation (3.3).
Compute $\delta J[\varphi_i](r_N)$, $i = 0, \dots, N$, using formula (3.5).
update r_N (steepest descent, conjugate gradients.)
until converged

6.1. Test problem with a known analytic solution

To illustrate the behavior of the optimization method we consider the source function

$$f(t) = \exp(t)$$

in (2.1). This function results in the well known solution $U(x, t) = \exp(t - x) - 1$ and interface position $R(t) = t$, which is compared with the numerical solution to assess error and convergence speed.

In this experiment the finite dimensional subspace consists of the polynomials of degree N that vanish for $t = 0$. The basis functions are expressed in terms of the Legendre polynomials P_j, specifically

$$\varphi_j(t) = t\, P_j\left(\frac{2}{T}\left(t - \frac{T}{2}\right)\right). \tag{6.2}$$

The coefficients of the exact interface position in (6.1) are $a_0 = 1$ and $a_j = 0, j > 0$. To test the iterative optimization we start with an initial guess and monitor the evolution of the coefficients as the minimization progresses. This is illustrated in Fig. 1. Since the *exact solution* $r(t)$ can be expanded with just one term in (6.1), the numerical solution does not improve if the degree N is increased and therefore it was fixed at $N = 5$. However, the approximation is dependent on the number of time intervals in the integral equation solver. Fig. 2 shows the error as a function of time for different step sizes, and Table 1 displays the final functional and the maximum error of $r(t)$. The data is consistent with the theoretical $O(M^{-\frac{3}{2}})$ convergence rate of the discretization method of the integral equation.

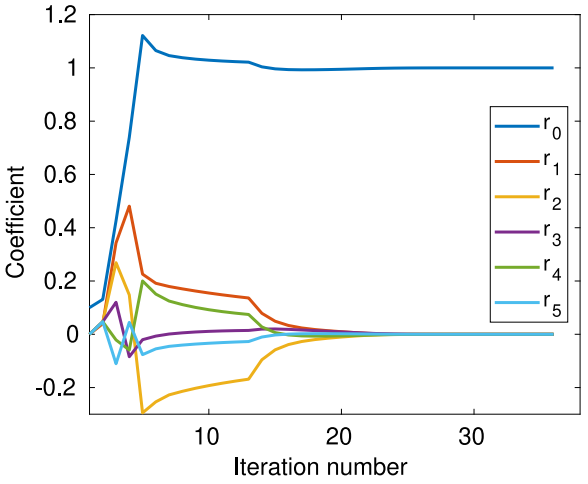

Fig. 1. Convergence of the coefficients in (6.1) in the iteration. Section 6.1.

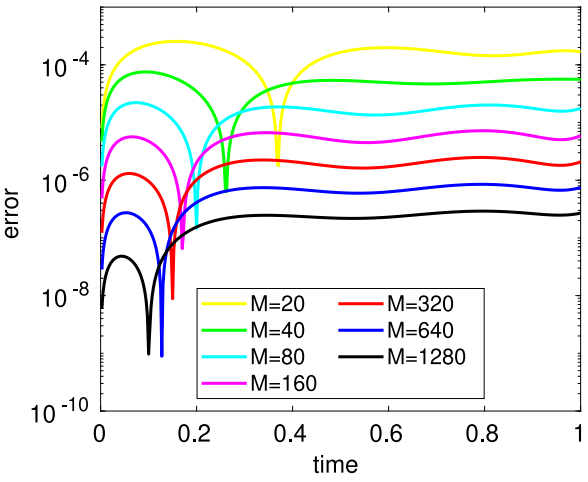

Fig. 2. Error of the interface position for different numbers of time steps M. Section 6.1.

6.2. Switching off the source term

The second example has the source term

$$f(t) = \begin{cases} 1, & 0 \le t \le \frac{1}{2}, \\ 0, & \frac{1}{2} \le t. \end{cases}$$

Here the analytical solution is not known, but it is not difficult to determine that the interface will monotonically converge to the final value

$$R_\infty = \int_0^{\frac{1}{2}} f(t)\,dt = \frac{1}{2}.$$

We compute the numerical solution using the Legendre basis (6.2) and the discretization parameters of Table 2, which also shows the CPU times obtained with an off the shelf desktop computer. Since the exact solution $R(t)$ is not a polynomial, the degree in (6.1) must be increased together with the number of time steps of the integral equation solution. Assuming an analytic $R(t)$, the approximation by Legendre functions is exponential and therefore an algebraic progression of the degree suffices when halving the time step size of the integral equation solver.

The interface of the second problem is more challenging to approximate with Legendre polynomials because of the fact that $R(t)$ approaches a constant value. Another choice of φ_i's would be more suitable, but the point here is to demonstrate the robustness of the minimization with respect to the basis. One can see that in the resolution of Fig. 3, the second coarsest mesh is already difficult to distinguish from the finer solutions. Fig. 4 displays the convergence history of the

Table 2
Discretization parameters and CPU times for the example in Section 6.2. M is the number of time steps in the integral equation solver.

M	Degree	cpu (s)
80	4	–
160	8	1
320	12	4
640	16	15
1280	20	60

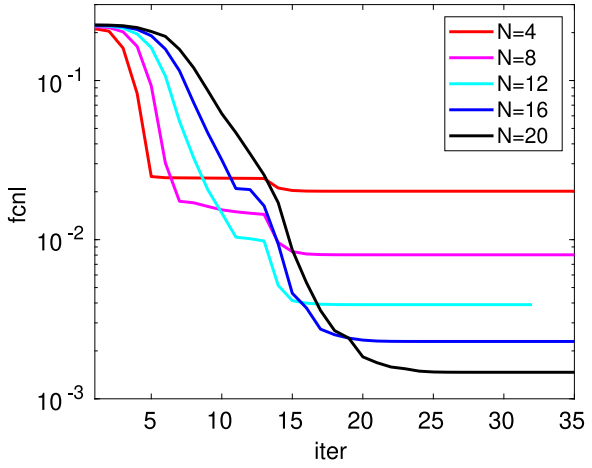

Fig. 3. Convergence of the error functional for different degrees of $r_N(t)$. Section 6.2.

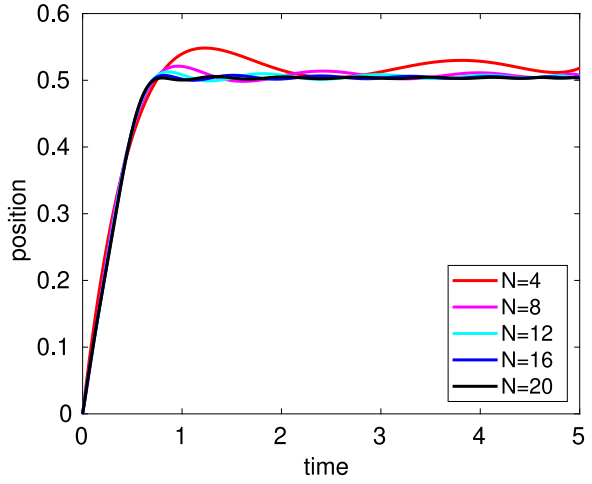

Fig. 4. Interface position for different degrees of $r_N(t)$. Second example.

shape functional for the different meshes. It is apparent that the convergence rate is mildly dependent on the chosen mesh. For the finest mesh the functional became stationary after approximately 25 iterations.

6.3. Oscillatory source term

The last example has the source term

$$f(t) = \begin{cases} 1, & 0 \le t \le \frac{\pi}{2}, \\ \sin(t), & \frac{\pi}{2} \le t. \end{cases}$$

Table 3
Discretization parameters and CPU times for the example in Section 6.3.

N	M	cpu (s)
320	3200	404
640	6400	2187
1280	12 800	8769

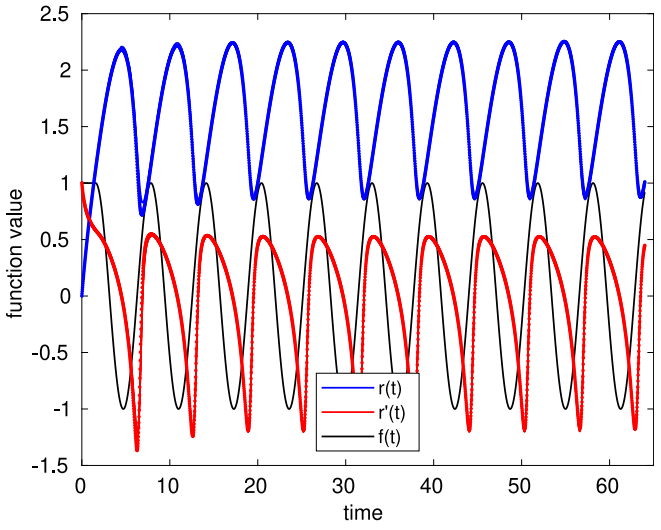

Fig. 5. Interface position $r(t)$, speed $r'(t)$ and force term $f(t)$ for the example in Section 6.3.

This source term is oscillatory except for a short initial warm up time which is necessary to move the interface away from the origin. While the exact interface position is unknown, it can be determined that it will oscillate between two fixed values in the limit as $t \to \infty$. Since the Legendre basis is not suitable to approximate such a behavior we use instead the cubic spline basis

$$\varphi_j(t) = \begin{cases} -B_3(t/h_s + 1) + \frac{1}{4}B_3(t/h_s), & j = 0, \\ B_3(t/h_s - 1) + \frac{1}{4}B_3(t/h_s), & j = 1, \\ B_3(t/h_s - j), & j = 2, \ldots, N+1. \end{cases}$$

Here B_3 is the cardinal cubic B-Spline, h_s is the spacing between the nodes, $N = T/h_s$, and the functions defined above are restricted to the interval $[0, T]$. The first two functions φ_0 and φ_1 are defined such that the homogeneous initial condition is satisfied.

We have computed the interface position for $T = 64$, which implies that the interval contains about ten oscillations of the source term. In this experiment we used three refinements. Table 3 gives the details about number of nodes in the spline basis, time steps of the integral equation solver as well as the total CPU time to solve the optimization problem.

Fig. 5 displays the numerically computed interface positions, the derivative and the source term. This plot displays all three refinements, but the numerical solutions are so close that they mostly overlap in the resolution of this figure. The CPU time is roughly proportional to M^2, which is the asymptotic cost of the integral equation solver.

7. Conclusion

We have formulated the classical Stefan problem as a shape optimization problem and solved the state and adjoint equation using an integral equation formulation. We were able to show that the shape functional is only stationary at the optimal solution, a property that is rarely seen in shape optimization. Our implementation indicates that the convergence of the interface position is consistent with the convergence of ansatz function space and quadrature order of the Nyström discretization of the integral equation. The dominant cost is to solve the integral equations which has $O(M^2)$-complexity using the direct approach. However, fast evaluation methods could be used to reduce this to nearly $O(M)$-complexity, see [25]. For the one-dimensional case considered here, this is not really necessary since our most complex example took less than 2.5 h to solve. However, a future research direction is to extend the shape optimization approach to Stefan problems in more space dimensions. Here, fast evaluation methods of parabolic boundary integral operators will be important to make the presented approach applicable to significant applications.

References

[1] J. Crank, Free and Moving Boundary Problems, Clarendon Press, 1984.
[2] S.C. Gupta, The Classical Stefan Problem, Basic Concepts, Modelling and Analysis with Quasi-Analytical Solutions and Methods, second ed., Elsevier, 2017.
[3] L.I. Rubinstein, The Stefan Problem, AMS, 1971.
[4] G.H. Meyer, One-dimensional parabolic free boundary problems, SIAM Rev. 19 (1) (1977) 17–34.
[5] S. Kutluay, A.R. Bahadir, A. Özdeş, The numerical solution of one-phase classical Stefan problem, J. Comput. Appl. Math. 81 (1997) 135–144.
[6] F. Liu, D.L.S. McElwain, A computationally efficient solution technique for moving-boundary problems in finite media, IMA J. Appl. Math. 59 (1999) 71–84.
[7] S.L. Mitchell, T.G. Myers, Application of standard and refined heat balance integral methods to one-dimensional Stefan problems, SIAM Rev. 52 (1) (2010) 57–86.
[8] H. Sha, K. Schwerdtfeger, Computation of the solidification of pure metals in plate geometry using Green's function method, Int. J. Heat Mass Transfer 41 (1998) 3226–3278.
[9] E. Case, J. Tausch, An integral equation method for spherical Stefan problems, Appl. Math. Comput. 218 (23) (2012) 11451–11460.
[10] J.A. Sethian, J. Strain, Crystal growth and dendritic solidification, J. Comput. Phys. 98 (2) (1992) 231–253.
[11] S. Chen, B. Merriman, S. Oscher, P. Smereka, A simple level set method for solving Stefan problems, J. Comput. Phys. 135 (1997) 8–29.
[12] J.P. Zolesio, M.C. Delfour, Shapes and Geometries. Metrics, Analysis, Differential Calculus, and Optimization, SIAM, 2011.
[13] J. Haslinger, R. Mäkinen, Introduction to Shape Optimization, SIAM, 2003.
[14] O. Pironneau, Optimal Shape Design for Elliptic Systems, Springer, 1983.
[15] J. Haslinger, T. Kozubek, K. Kunisch, G. Peichl, Shape optimization and fictitious domain approach for solving free boundary problems of Bernoulli type, Comput. Optim. Appl. 26 (2003) 231–251.
[16] K. Eppler, H. Harbrecht, R. Schneider, On convergence in elliptic shape optimization, SIAM J. Control Optim. 46 (1) (2007) 61–83.
[17] K. Eppler, H. Harbrecht, Tracking Neumann data for stationary free boundary problems, SIAM J. Control Optim. 48 (5) (2009) 2901–2916.
[18] H. Harbrecht, J. Tausch, An efficient numerical method for a shape identification problem arising from the heat equation, Inverse Problems 27 (6) (2011) 065013.
[19] H. Harbrecht, J. Tausch, On the solution of a shape optimization problem for the heat equation, SIAM J. Sci. Comput. 35 (1) (2013) A104–A121.
[20] R. Chapko, R. Kress, J.-R. Yoon, On the numerical solution of an inverse boundary value problem for the heat equation, Inverse Problems 14 (1998) 853–867.
[21] S.P. Ohezin, Optimal Shape Design for Parabolic System and Two-Phase Stefan Problem, in: International Series of Numerical Mathematics, vol. 106, Birkhäuser, 1992, pp. 239–244.
[22] D. Andreucci, Lecture Notes on the Stefan Problem, Tech. Rep., Università di Roma La Sapienza, 2005.
[23] A. Friedman, Remarks on the maximum principle for parabolic equations and its applications, Pacific J. Math. 8 (2) (1958) 201–211.
[24] J. Tausch, Nyström Discretization of parabolic boundary integral equations, Appl. Numer. Math. 59 (11) (2009) 2843–2856.
[25] J. Tausch, Fast Nyström methods for parabolic boundary integral equations, in: U. Langer, M. Schanz, O. Steinbach, W. Wendland (Eds.), Fast Boundary Element Methods in Engineering and Industrial Applications, in: Lecture Notes in Applied and Computational Mechanics, vol. 63, Springer, 2011, pp. 185–219.